

An Extended Electromotive Force Model for Sensorless Control of Interior Permanent-Magnet Synchronous Motors

Zhiqian Chen, *Member, IEEE*, Mutuwo Tomita, *Member, IEEE*, Shinji Doki, *Member, IEEE*, and Shigeru Okuma, *Member, IEEE*

Abstract—During the last decade, many sensorless control methods have been proposed for surface permanent-magnet synchronous motors (SPMSMs) based on estimation of electromotive force (EMF) in which the motor's position information is contained. However, these methods cannot be applied to interior PMSMs (IPMSMs) directly, because the position information is contained in not only the EMF, but also the inductance of stators. In this paper, a new mathematical model for IPMSMs is proposed and an extended EMF is defined, which includes both position information from the EMF and the stator inductance. By using the newly proposed model, sensorless controls proposed for SPMSMs can easily be applied to IPMSMs. As an example, a disturbance observer is studied and the experimental results show that the proposed method on the proposed model is very effective.

Index Terms—Disturbance observer, electromotive force (EMF), permanent-magnet synchronous motor (PMSM), sensorless control.

I. INTRODUCTION

PERMANENT-MAGNET synchronous motors (PMSMs) have been widely used as servo motors for their high performance and high efficiency. To control the PMSMs, rotor position and velocity knowledge are necessary. However, sensors for detection of these signals are expensive and mechanically bulky. Therefore, the position and velocity sensorless control has been desired.

To estimate the position and velocity of the PMSMs, the motor's mathematical model can be used. During the last decade, many sensorless control methods for surface PMSMs (SPMSMs) based on the motor's mathematical model have been proposed [1]–[3]. The basic idea of these methods is to estimate the permanent magnet's flux or electromotive force (EMF), because the rotor's position information is contained in these physical variables. The authors also proposed a disturbance observer for the EMF estimation of which stability is clarified by using a linear state equation [4].

However, these methods for SPMSMs cannot be used directly to interior PMSMs (IPMSMs). The mathematical model of SPMSMs is a special case of IPMSMs, and is relatively easy for mathematical procession. In the model of IPMSMs, position information is contained not only in the flux or the EMF term but also in the inductance because of their saliency [5]. To apply the methods for SPMSMs to a wide class of motors, i.e., IPMSMs, some extension should be made.

To solve this problem, some attempts have been made [6]–[8]. In [6] and [7], observers based on the rotating coordinates have been proposed. This is a simple approach as the IPMSMs' mathematical model on the rotating coordinate has similar structure to the SPMSMs' one. However, because the real rotating coordinate is unknown, approximations were made and this may destroy the stability of the sensorless control system under certain conditions.

In [8], two unique voltages are defined and by calculating these voltages, it is possible to obtain the rotor position and velocity. However, the authors did not give a clear physical meaning of the voltages. Also, there were derivation errors in defining the voltages. Besides, currents are differentiated in calculating the voltages, which makes the estimation sensitive to measurement noises.

By injecting some test signals, several methods have been proposed for the sensorless control of IPMSMs [5], [9]. However, because unwanted torque may be generated by the test signals, these methods are mostly used at low speeds and standstill. At high speeds, sensorless control without using test signals is necessary. Furthermore, because these methods cannot be used for SPMSMs, a unified method for all the PMSMs is still desired.

In this paper, a new mathematical model of IPMSMs is proposed and an extended EMF (EEMF) is defined. The EEMF contains the position information of not only in the conventionally defined EMF but also in the stator inductance. This makes it possible to obtain the rotor position and velocity by just estimating the EEMF. Because it is a general form of mathematical model for all the synchronous motors including SPMSMs, IPMSMs, and synchronous reluctance motors (SynRMs), a unified sensorless control method for all the synchronous motors at high speeds becomes possible. Using the proposed new model, sensorless control methods for the SPMSMs can be easily extended to the IPMSMs. As an example, the disturbance observer for an SPMSM in [4] is applied to an IPMSM. Experimental results show that the proposed method is very effective.

Manuscript received August 31, 2001; revised June 27, 2002. Abstract published on the Internet February 4, 2003.

Z. Chen and S. Okuma are with the Okuma Laboratory, Department of Electrical Engineering, Nagoya University, Nagoya 464-8603, Japan (e-mail: zqchen@ieee.org).

M. Tomita is with the Department of Electrical and Computer Engineering, Gifu National College of Technology, Gifu 501-0495, Japan.

S. Doki is with the Department of Electrical Engineering, Mie University, Tsu 514-8507, Japan.

Digital Object Identifier 10.1109/TIE.2003.809391

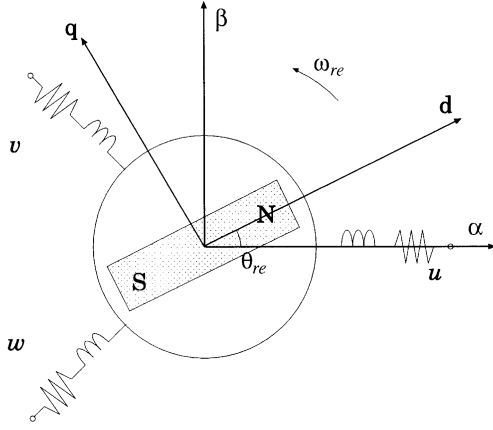


Fig. 1. Coordinates of PMSMs.

II. MATHEMATICAL MODELS

In this section, circuit equations of PMSMs, which are used as mathematical models for sensorless control, are discussed on two kinds of coordinates. These coordinates are the d - q rotating coordinate and the α - β fixed coordinate, which are defined in Fig. 1.

A. Mathematical Model of SPMSMs

The circuit equation of SPMSMs on the d - q rotating coordinate is given by (1)

$$\begin{bmatrix} v_d \\ v_q \end{bmatrix} = \begin{bmatrix} R + pL & -\omega_{re}L \\ \omega_{re}L & R + pL \end{bmatrix} \begin{bmatrix} i_d \\ i_q \end{bmatrix} + \begin{bmatrix} 0 \\ \omega_{re}K_E \end{bmatrix} \quad (1)$$

where

$\begin{bmatrix} v_d & v_q \end{bmatrix}^T$	voltage on rotating frame;
$\begin{bmatrix} i_d & i_q \end{bmatrix}^T$	current on rotating frame;
R	stator resistance;
L	stator inductance;
p	differential operator;
K_E	EMF constant;
ω_{re}	angular velocity at electrical angle;
θ_{re}	rotor position at electrical angle.

The first term on the right side of (1) is a voltage drop on the motor's impedance, and the second term is an EMF term.

Transforming (1) on the α - β fixed coordinate, (2) is derived

$$\begin{bmatrix} v_\alpha \\ v_\beta \end{bmatrix} = \begin{bmatrix} R + pL & 0 \\ 0 & R + pL \end{bmatrix} \begin{bmatrix} i_\alpha \\ i_\beta \end{bmatrix} + \omega_{re}K_E \begin{bmatrix} -\sin \theta_{re} \\ \cos \theta_{re} \end{bmatrix} \quad (2)$$

where $\begin{bmatrix} v_\alpha & v_\beta \end{bmatrix}^T = v$ is the voltage on the fixed coordinate, and $\begin{bmatrix} i_\alpha & i_\beta \end{bmatrix}^T = i$ is the current on the fixed coordinate. From (2), it is known that the rotor position information is contained in the EMF term. By estimating the EMF, it is possible to get θ_{re} from its phase.

The physical meaning of sensorless estimation can be interpreted by Fig. 2(a). The stator voltage v is a sum of three voltage vectors, A , B , and C , which correspond to three terms on the right side of (3), which is rewritten from (2). Here, suppose that the stator voltage v and current i can be detected by sensors. Then, the voltage drops A on resistance and B on inductance can be calculated from the current i , nominal values of the re-

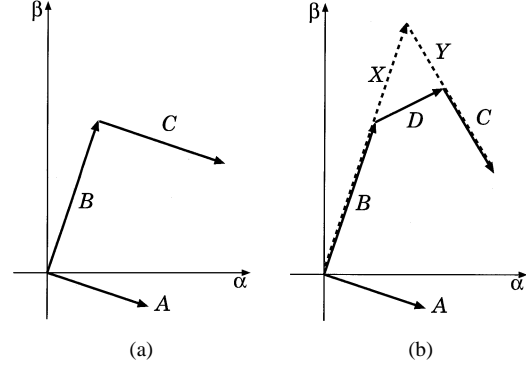


Fig. 2. Vector diagrams of (a) SPMSMs and (b) IPMSMs.

sistance R and the inductance L . Therefore, the only unknown variable is the EMF term C . Therefore, the vector C can be obtained from (3)

$$\begin{bmatrix} v_\alpha \\ v_\beta \end{bmatrix} = \underbrace{R \begin{bmatrix} i_\alpha \\ i_\beta \end{bmatrix}}_A + \underbrace{pL \begin{bmatrix} i_\alpha \\ i_\beta \end{bmatrix}}_B + \underbrace{\omega_{re}K_E \begin{bmatrix} \sin \theta_{re} \\ \cos \theta_{re} \end{bmatrix}}_C. \quad (3)$$

B. Mathematical Model of IPMSM

The circuit equation of IPMSMs on the d - q rotating coordinate is given by (4)

$$\begin{bmatrix} v_d \\ v_q \end{bmatrix} = \begin{bmatrix} R + pL_d & -\omega_{re}L_q \\ \omega_{re}L_d & R + pL_q \end{bmatrix} \begin{bmatrix} i_d \\ i_q \end{bmatrix} + \begin{bmatrix} 0 \\ \omega_{re}K_E \end{bmatrix} \quad (4)$$

where L_d is the inductance of the d axis, and L_q is the inductance of the q axis. Transforming (4) on the α - β fixed coordinate, (5) is derived

$$\begin{bmatrix} v_\alpha \\ v_\beta \end{bmatrix} = \begin{bmatrix} R + pL_\alpha & pL_{\alpha\beta} \\ pL_{\alpha\beta} & R + pL_\beta \end{bmatrix} \begin{bmatrix} i_\alpha \\ i_\beta \end{bmatrix} + \omega_{re}K_E \begin{bmatrix} -\sin \theta_{re} \\ \cos \theta_{re} \end{bmatrix} \quad (5)$$

where

$$\begin{aligned} L_\alpha &= L_0 + L_1 \cos 2\theta_{re} \\ L_\beta &= L_0 - L_1 \cos 2\theta_{re} \\ L_{\alpha\beta} &= L_1 \sin 2\theta_{re} \\ L_0 &= \frac{(L_d + L_q)}{2} \\ L_1 &= \frac{(L_d - L_q)}{2}. \end{aligned}$$

Equation (5) is obviously different from (2) in that both $2\theta_{re}$ and θ_{re} terms are contained, which is not easy for mathematical procession. This can be interpreted by Fig. 2(b). The vectors A , B , C , and D correspond to terms on the right side of (6), which is rewritten from (5). However, at this time, there are two unknown vectors, C and D , having functions of the rotor position θ_{re} , which makes the equation difficult to solve

$$\begin{bmatrix} v_\alpha \\ v_\beta \end{bmatrix} = \underbrace{R \begin{bmatrix} i_\alpha \\ i_\beta \end{bmatrix}}_A + \underbrace{pL_0 \begin{bmatrix} i_\alpha \\ i_\beta \end{bmatrix}}_B + \underbrace{\omega_{re}K_E \begin{bmatrix} \sin \theta_{re} \\ \cos \theta_{re} \end{bmatrix}}_C + \underbrace{pL_1 \begin{bmatrix} \cos 2\theta_{re} & \sin 2\theta_{re} \\ \sin 2\theta_{re} & -\cos 2\theta_{re} \end{bmatrix} \begin{bmatrix} i_\alpha \\ i_\beta \end{bmatrix}}_D. \quad (6)$$

An easy way to solve this equation is to use the estimated position $\hat{\theta}_{re}$ instead of θ_{re} to calculate vector D . This is possible if the amplitude of D is smaller enough than C , i.e., $[L_1 i] \ll K_E$. The approximation made in [6] and [7] is based on the assumption that this condition is valid.

This condition is true for those motors with relatively small reluctance torque. However, if the motor's reluctance torque cannot be neglected compared with the permanent-magnet torque, the sensorless estimation may be unstable [10].

However, it is possible to eliminate the $2\theta_{re}$ terms in (5). It is known that there is no secondary harmonic component in the motor current if higher order harmonic voltages generated by an inverter are neglected. Therefore, it is natural to think about elimination of the $2\theta_{re}$ terms by some purely mathematical methods.

Comparing (4) with (1), a reason why $2\theta_{re}$ terms appear can be concluded as that the impedance matrix in (4) is asymmetrical. If the impedance matrix is rewritten symmetrically like

$$\begin{bmatrix} v_d \\ v_q \end{bmatrix} = \begin{bmatrix} R + pL_d & -\omega_{re}L_q \\ \omega_{re}L_q & R + pL_d \end{bmatrix} \begin{bmatrix} i_d \\ i_q \end{bmatrix} + \begin{bmatrix} 0 \\ (L_d - L_q)(\omega_{re}i_d - \dot{i}_q) + \omega_{re}K_E \end{bmatrix} \quad (7)$$

the circuit equation on the α - β coordinate can be derived as (8), in which there is no $2\theta_{re}$ term

$$\begin{bmatrix} v_\alpha \\ v_\beta \end{bmatrix} = \begin{bmatrix} R + pL_d & \omega_{re}(L_d - L_q) \\ -\omega_{re}(L_d - L_q) & R + pL_d \end{bmatrix} \begin{bmatrix} i_\alpha \\ i_\beta \end{bmatrix} + \{(L_d - L_q)(\omega_{re}i_d - \dot{i}_q) + \omega_{re}K_E\} \begin{bmatrix} -\sin\theta_{re} \\ \cos\theta_{re} \end{bmatrix}. \quad (8)$$

The differential operator “ \cdot ” in the second term on the right side of (8) means that it is only effective for i_q , and that it is not effective for the following $\sin\theta_{re}$ and $\cos\theta_{re}$. This usage is different from the differential operator p used in (4)

$$\begin{bmatrix} v_\alpha \\ v_\beta \end{bmatrix} = \underbrace{R \begin{bmatrix} i_\alpha \\ i_\beta \end{bmatrix}}_A + \underbrace{\begin{bmatrix} pL_d & \omega_{re}(L_d - L_q) \\ -\omega_{re}(L_d - L_q) & pL_d \end{bmatrix} \begin{bmatrix} i_\alpha \\ i_\beta \end{bmatrix}}_X + \underbrace{\{(L_d - L_q)(\omega_{re}i_d - \dot{i}_q) + \omega_{re}K_E\} \begin{bmatrix} -\sin\theta_{re} \\ \cos\theta_{re} \end{bmatrix}}_Y. \quad (9)$$

The second term and third term on the right side of (9), which is rewritten from (8), are depicted in Fig. 2(b) as vectors X and Y in dashed lines, respectively. They can be explained as extensions of the vectors B , C with decomposition of the vector D in their directions. Here, X has no relation to rotor position θ_{re} so that Y becomes the only vector having functions of θ_{re} . This makes the sensorless estimation problem of IPMSMs as easy to be solved as that of SPMSMs.

The second term on the right side of (8) is defined as an EEMF by (10). In this term, besides the conventionally defined EMF generated by the permanent magnet, there is a kind of voltage related to the saliency of the IPMSM. It includes the position information from both the EMF and the stator inductance. If the

EEMF can be estimated, then the position of the magnet can be obtained from its phase just like the EMF in SPMSMs

$$e = \begin{bmatrix} e_\alpha \\ e_\beta \end{bmatrix} = \{(L_d - L_q)(\omega_{re}i_d - \dot{i}_q) + \omega_{re}K_E\} \begin{bmatrix} -\sin\theta_{re} \\ \cos\theta_{re} \end{bmatrix}. \quad (10)$$

Equation (8) is an equivalent transformation of (5) without any approximation. It is a general form of mathematical model for all the synchronous motors. When $L_d = L_q$, it reduces into the equation of SPMSMs, and when $K_E = 0$, it becomes the equation of SynRMs. Based on this model, it is easy to apply sensorless control methods proposed for SPMSMs to IPMSMs. Also, it is reasonable to think that those methods are valid for SynRMs.

There is a differential term of i_q in the EEMF. This means that even when the motor's velocity is near zero, the EEMF e is not zero if the q -axis current i_q is changing. This property will be useful for standstill and low-speed drives.

III. DISTURBANCE OBSERVER

Regarding the EEMF in (8) as a disturbance, the EEMF can be estimated by a disturbance observer for medium- and high-speed drives. This method was first proposed for SPMSMs [4]. With the new model of (8), it becomes applicable to IPMSMs.

The observer is based on a linear state equation, so that linear control theory can be used in the design of the observer to guarantee stability and robustness.

A. Linear State Equation

From the new model of (8), the IPMSM can be described by a linear state equation as (11) [11]. Here, the state variables are stator current i and EEMF e . The system's input is the stator voltage v and output is the stator current i . Assuming that the electrical system's time constant is smaller enough than the mechanical one, the velocity ω_{re} is regarded as a constant parameter

$$p \begin{bmatrix} i \\ e \end{bmatrix} = \begin{bmatrix} A_{11} & A_{12} \\ 0 & A_{22} \end{bmatrix} \begin{bmatrix} i \\ e \end{bmatrix} + \begin{bmatrix} B_1 \\ 0 \end{bmatrix} v + \begin{bmatrix} 0 \\ W \end{bmatrix} \quad (11)$$

$$i = C \cdot \begin{bmatrix} i \\ e \end{bmatrix}$$

where

$$A_{11} = -\left(\frac{R}{L_d}\right)I + \left\{\omega_{re}\frac{(L_d - L_q)}{L_d}\right\}J$$

$$A_{12} = \left(\frac{-1}{L_d}\right)I = a_{12}I$$

$$A_{22} = \omega_{re}J = a_{22}J$$

$$B_1 = \left(\frac{1}{L_d}\right)I$$

$$C = [I \quad 0]$$

$$W = (L_d - L_q)(\omega_{re}i_d - \dot{i}_q) \begin{bmatrix} -\sin\theta_{re} \\ \cos\theta_{re} \end{bmatrix}$$

$$I = \begin{bmatrix} 1 & 0 \\ 0 & 1 \end{bmatrix}$$

$$J = \begin{bmatrix} 0 & -1 \\ 1 & 0 \end{bmatrix}.$$

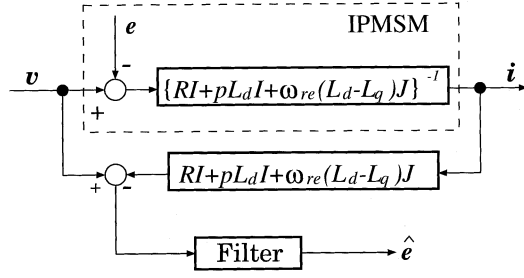


Fig. 3. Configuration of disturbance observer.

The W term in (11) is a linearization error. This term appears only when i_d or i_q is changing. However, under the velocity control this happens in a very short time because of the high response of the current control loop. Besides, the proposed disturbance observer has an embedded low-pass filter which can cut off the effect of W .

B. Configuration of Disturbance Observer

To estimate the state e in a system described by (11), a reduced-order observer is constructed as (12)

$$\begin{aligned}\dot{\hat{i}} &= \tilde{A}_{11}\hat{i} + \tilde{A}_{12}\hat{e} + \tilde{B}_1v \\ \dot{\hat{e}} &= \tilde{A}_{22}\hat{e} + G(\hat{i} - i) \\ &= G\tilde{A}_{11}\hat{i} + G(\tilde{A}_{12} + \tilde{A}_{22})\hat{e} + G\tilde{B}_1v - G\dot{i}\end{aligned}\quad (12)$$

where

- $\hat{\cdot}$ estimated state variable;
- $\tilde{\cdot}$ parameter's nominal value;
- $G = g_1I + g_2J$ feedback gain.

To avoid differentiation of current i , an intermediate variable ξ is introduced as (13)

$$\begin{aligned}\xi &= \hat{e} + Gi \\ \dot{\xi} &= \dot{\hat{e}} + G\dot{i}.\end{aligned}\quad (13)$$

Substituting (13) into (12) yields (14)

$$\begin{aligned}\dot{\xi} &= (G\tilde{A}_{12} + \tilde{A}_{22})\xi + G\tilde{B}_1v + (G\tilde{A}_{11}I - G\tilde{A}_{12}G - \tilde{A}_{22}G)\hat{i} \\ \hat{e} &= \xi - Gi.\end{aligned}\quad (14)$$

This is an equivalent disturbance observer as shown in Fig. 3, where the filter's frequency response function $H(j\omega)$ is as (15)

$$H(j\omega) = \{\alpha I + (\omega_{re} - \beta)J\} \frac{(j\omega + \alpha)I + \beta J}{(j\omega + \alpha)^2 + \beta^2} \quad (15)$$

and α, β are the observer's poles having the following relation with the observer gain G :

$$\begin{aligned}\alpha &= -g_1a_{12} \\ \beta &= a_{22} + g_2a_{12}.\end{aligned}$$

C. Pole Assignment of Disturbance Observer

The poles of the disturbance observer are assigned under two considerations. One is for robust EEMF estimation against velocity estimation error. The other is for suppression of harmonic components in EMF.

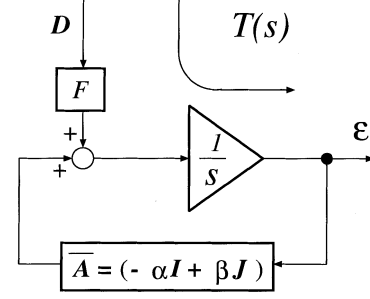


Fig. 4. Block diagram of error equation.

In the proposed disturbance observer, velocity ω_{re} is used as a parameter. However, the real value of ω_{re} is unknown and the estimated one $\hat{\omega}_{re}$ is used instead. At accelerations and decelerations, transient velocity estimation error is inevitable. This may cause EEMF estimation error, and EEMF estimation error may lead to more velocity estimation error [12].

To stop this vicious spiral, the EEMF estimation should be robust against velocity estimation error. In this section, a pole assignment to make the disturbance observer robust is described.

From (11) and (12), considering there is no parameter deviations except for the velocity estimation error $\Delta\omega_{re} = \hat{\omega}_{re} - \omega_{re}$ so that $\tilde{A}_{12} = A_{12}$ and $\tilde{B}_1 = B_1$, the observer's error equation is derived as (16)

$$\begin{aligned}\dot{\epsilon} &= (\tilde{A}_{22} + GA_{12})\epsilon + [G(\tilde{A}_{11} - A_{11})\tilde{A}_{22} - A_{22}] \begin{bmatrix} i \\ e \end{bmatrix} \\ &= (-\alpha I + \beta J)\epsilon + FD \\ &= \bar{A}\epsilon + FD\end{aligned}\quad (16)$$

where $\epsilon = \hat{e} - e$ is the EEMF estimation error. The normalized disturbance vector D and its input matrix F are defined as follows. Here, I_m is the amplitude of the stator current i

$$\begin{aligned}D &= \begin{bmatrix} \frac{i}{I_m} & \frac{e}{\omega_{re}K_E} \end{bmatrix}^T \Delta\omega_{re} \\ F &= [(L_d - L_q)\{\alpha I + (\beta - \hat{\omega}_{re})J\} I_m \quad \omega_{re}K_E I] J.\end{aligned}$$

The error equation's block diagram is shown in Fig. 4. From the figure, the feedback gain G , or the closed-loop poles $(-\alpha, \beta)$, decide not only the response of the EEMF estimation, but also the input matrix of the disturbance.

Let the transfer function from the disturbance vector D to the EEMF estimation error ϵ be $T(s)$. $T(s)$ is defined as

$$T(s) = (sI - \bar{A})^{-1}F. \quad (17)$$

The influence of the velocity estimation error $\Delta\omega_{re}$ can be evaluated by the H_∞ norm of $T(s)$

$$\begin{aligned}\|T\|_\infty &= \sup_{\omega} \sigma_{\max}[T(j\omega)] \\ &= \sup_{\omega} \sqrt{\lambda_{\max}[T^H(j\omega) \cdot T(j\omega)]} \\ &\leq \sup_{\omega} \frac{\|F\|_2}{\sqrt{(\omega - |\beta|)^2 + \alpha^2}} \\ &= \frac{\|F\|_2}{\alpha} \text{ (at } \omega = |\beta| \text{)}\end{aligned}\quad (18)$$

where

- $\sigma_{\max}[\cdot]$ maximum singular value;
- $\lambda_{\max}[\cdot]$ maximum eigenvalue;
- $(\cdot)^H$ complex conjugate transposition;
- $\|\cdot\|_2$ induced norm.

The induced norm of F is calculated as

$$\begin{aligned} \|F\|_2 &= \sigma_{\max}[F] \\ &= \sqrt{(L_d - L_q)^2 I_m^2 \{\alpha^2 + (\beta - \hat{\omega}_{re})^2\} + (\omega_{re} K_E)^2}. \end{aligned} \quad (19)$$

From (19), the best β assignment which makes $\|F\|_2$ minimum is

$$\beta = \hat{\omega}_{re}. \quad (20)$$

Then, (18) becomes

$$\begin{aligned} \|T\|_\infty &\leq \sqrt{(L_d - L_q)^2 I_m^2 + \left(\frac{\omega_{re} K_E}{\alpha}\right)^2} \\ &\leq \sqrt{(L_d - L_q)^2 I_{\max}^2 + \left(\frac{\omega_{re} K_E}{\alpha}\right)^2} \\ &\leq \nu'_1 \end{aligned} \quad (21)$$

where I_{\max} is the maximum current and ν'_1 is a free parameter for robust estimation which can be decided by manual tuning.

According to (21), the assignment of the pole α which makes the EEMF estimation robust against velocity estimation error is derived as

$$\alpha \geq |\omega_{re}| \nu_1 \quad (22)$$

where the relation between ν_1 and ν'_1 can be calculated from (21) as

$$\nu' = \frac{K_E}{\sqrt{\nu_1'^2 - (L_d - L_q)^2 I_{\max}^2}}. \quad (23)$$

From (22), the lower limit of the pole α for robust velocity estimation is decided. However, an unlimited high gain is not desired, either. Next, the decision of the higher limit of the pole α will be discussed in consideration of higher harmonic component suppression.

Usually, for salient-pole motors such as IPMSMs and SynRMs, there are higher harmonic components in EMF because of interactions between the stator teeth and the permanent magnet or the rotor teeth. The frequency of the harmonic are decided by the motor structure. For an example, the motor in our experimental system has 24 slots and two pairs of poles, so 12th harmonic component is contained in the EMF as in Fig. 5.

These kinds of higher harmonic components in EMF may spoil the accuracy of position estimation. Using the embedded filter in the disturbance observer of Fig. 3 with the response function as (15), it is possible to get rid of them.

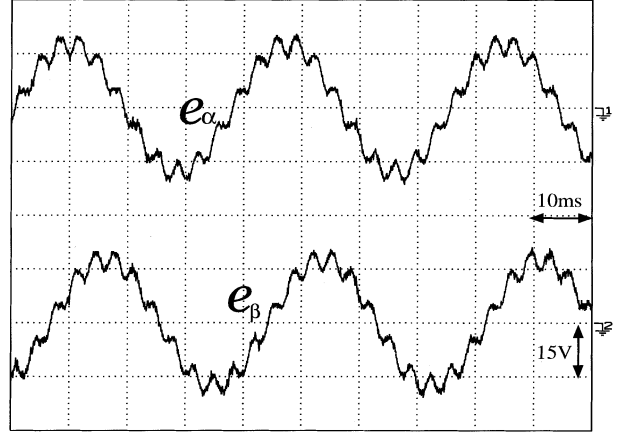


Fig. 5. 12th harmonic component in EMF.

Considering (20), the induced norm of the frequency response function of the observer's embedded filter $\|H(j\omega)\|_2$ is calculated as (24)

$$\begin{aligned} \|H(j\omega)\|_2 &= \sigma_{\max}[H(j\omega)] \\ &= \sqrt{\lambda_{\max}[H^H(j\omega) \cdot H(j\omega)]} \\ &= \alpha \sqrt{\frac{\alpha^2 + (\omega + \omega_{re})^2}{(\alpha^2 + \omega_{re}^2 - \omega^2)^2 + 4(\alpha\omega)^2}}. \end{aligned} \quad (24)$$

The relative influence of the 12th harmonic component is evaluated by the ratio of the 12th harmonic component's induced norm $\|H(12j\omega_{re})\|_2$ to the fundamental harmonic component's one $\|H(j\omega_{re})\|_2$

$$\frac{\|H(12j\omega_{re})\|_2}{\|H(j\omega_{re})\|_2} \leq \nu'_2. \quad (25)$$

From (24) and (25), it is obvious that to make this possible at any velocity ω_{re} , the pole α should be as

$$\alpha \leq |\omega_{re}| \nu_2 \quad (26)$$

where ν_2 is a free parameter deciding the relative amplitude of the 12th harmonic component, which can be calculated from (25).

From the above, the poles assignment of the disturbance observer is decided as

$$\begin{aligned} \alpha &= |\omega_{re}| \nu, \quad \nu_1 \leq \nu \leq \nu_2 \\ \beta &= \hat{\omega}_{re}. \end{aligned} \quad (27)$$

IV. POSITION AND VELOCITY ESTIMATION

The rotor position and velocity can be calculated from the estimated EEMF \hat{e} . With the estimated position and velocity, the IPMSM can be controlled sensorlessly.

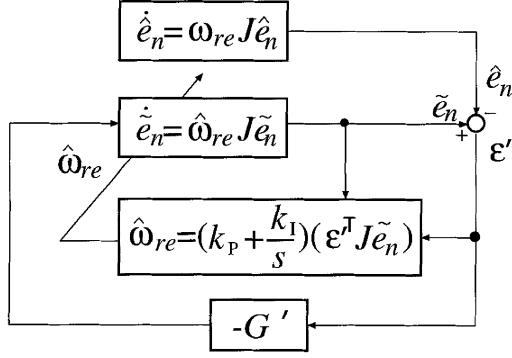


Fig. 6. Configuration of adaptive velocity estimator.

A. Position Estimation

Using the estimated value of the EEMF, the position is calculated as follows:

$$\hat{\theta}_{re} = \tan^{-1} \left(-\frac{\hat{e}_\alpha}{\hat{e}_\beta} \right). \quad (28)$$

Note that the amplitude of EEMF is not used for position estimation.

B. Adaptive Velocity Estimation

The rotor's velocity can be estimated by an adaptive velocity estimator [4]. The concept of the estimator is shown in Fig. 6.

First, the estimated EEMF is normalized as (29)

$$\hat{e}_n = \frac{1}{\sqrt{\hat{e}_\alpha^2 + \hat{e}_\beta^2}} \begin{bmatrix} \hat{e}_\alpha \\ \hat{e}_\beta \end{bmatrix}. \quad (29)$$

Then, for the normalized EEMF, the next equation is valid by assuming ω_{re} as a constant parameter

$$\dot{\hat{e}}_n = \omega_{re} J \hat{e}_n. \quad (30)$$

This equation is used as the reference model in the adaptive velocity estimator. Based on (30), the estimation model is defined as

$$\dot{\tilde{e}}_n = \hat{\omega}_{re} J \tilde{e}_n + G'(\tilde{e}_n - \hat{e}_n) \quad (31)$$

where \tilde{e}_n is the output of the estimation model and $\hat{\omega}_{re}$ is the estimated velocity. For convergence, a feedback loop is introduced and the feedback gain is $G' = g'I$.

If the velocity estimation error exists, it will lead to the normalized EEMF estimation error $\varepsilon' = \tilde{e}_n - \hat{e}_n$. Then, this error together with the estimation model's output \tilde{e}_n is used to calculate the velocity $\hat{\omega}_{re}$ by the adaptive scheme as (32)

$$\hat{\omega}_{re} = \left(k_p + \frac{k_I}{s} \right) (\varepsilon'^T J \tilde{e}_n). \quad (32)$$

The stability of the estimation is guaranteed by Popov's hyperstability theory so that the error ε' might converge to zero, and the estimated velocity $\hat{\omega}_{re}$ might converge to its real value ω_{re} at last [4].

TABLE I
PARAMETERS OF TEST MOTOR

Rated power	500	[W]
Rated current	5	[A]
Rated torque	1.2	[N·cm]
Stator resistance	R	0.45 [Ω]
Stator inductance	L_d	4.15 [mH]
	L_q	16.74 [mH]
Rotor inertia	J	0.06 [kg·cm·s ²]
Number of pole pairs	P	2
EMF constant	K_E	0.104 [V·s/rad]
DC link voltage	V_{DC}	130 [V]
Maximum current	I_{max}	14 [A]

TABLE II
PARAMETERS FOR CONTROLLER

Constant for observer's pole	ν	2
Estimator's feedback gain	g'	1000
Adaptive scheme gains	k_P	0.01 [rad/s/V ²]
	k_I	5000 [rad/s ² /V ²]
Velocity controller gains	k_{SP}	0.08 [A·s/rad]
	k_{SI}	0.7 [A/rad]

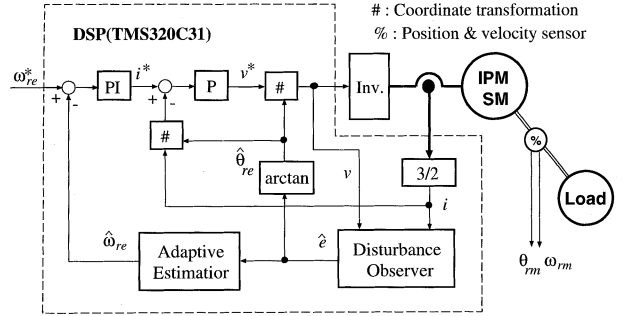


Fig. 7. Configuration of experimental system.

V. EXPERIMENTAL RESULTS

Using the proposed method, experiments of position- and velocity-sensorless velocity control were carried out on an IPMSM with parameters listed in Table I. The parameters for the controllers are listed in Table II. The configuration of the experimental system is shown in Fig. 7.

Currents and voltages are used in sensorless position and velocity estimation. The motor's stator currents are detected by sensors and then sent into a digital signal processor (DSP) TMS320C31 through 12-bit A/D converters. In the DSP program, three-phase current signals ($u-v-w$ coordinate) are converted into two-phase coordinate signals ($\alpha-\beta$ coordinate). For the voltages, the inverter's input commands v^* , not the voltage sensors, are used to reduce cost and influence of the sensor's offsets. At low speeds below 100 r/min, the actual voltage v 's amplitude and phase may be different from the voltage command v^* because of the influence of dead times. This is compensated by a simple lookup table and a low-pass filter based on experimental results.

At starting, a synchronized rotation is used to accelerate the motor to a certain speed and then the sensorless control starts.

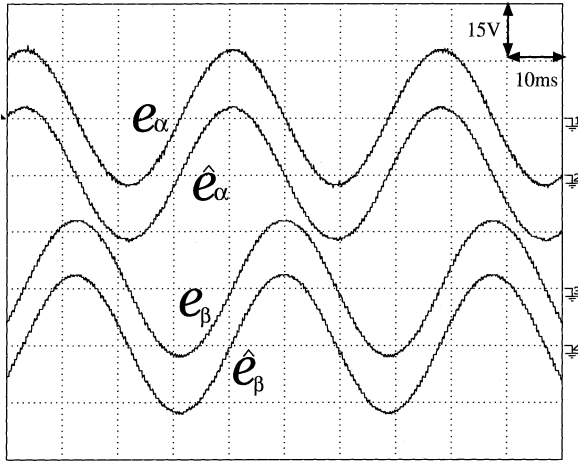


Fig. 8. Result of EEMF estimation.

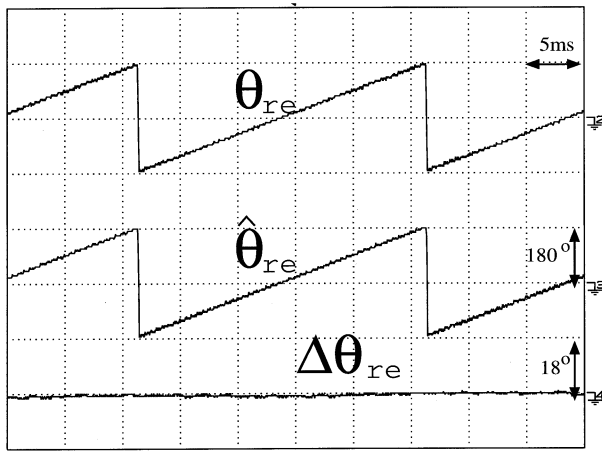


Fig. 9. Result of position estimation.

Using the current and the voltage signals, the EEMF \hat{e} is estimated by the proposed disturbance observer. The rotor position $\hat{\theta}_{re}$ is obtained from the phase of the estimated EEMF \hat{e} . The velocity $\hat{\omega}_{re}$ is estimated by the adaptive estimator. The difference between the velocity command ω_{re}^* and the estimated velocity $\hat{\omega}_{re}$ is used to generate current command i^* at the rotor reference frame (d - q coordinate) by the proportional plus integral (PI) controller in Fig. 7, so that maximum torque might be generated. At speeds higher than the rated one, field-weakening control is used. From i^* , the voltage command v^* is calculated by the current controller and then converted into the stator reference three-phase frame using the estimated rotor position $\hat{\theta}_{re}$. Then, the voltage command v^* is sent to the inverter to drive the motor. The pulsewidth modulation (PWM) inverter's maximum switching frequency is 5 kHz. A 1.5-kW SPMSM is used as load. An absolute encoder is used to detect the rotor position and velocity for verification.

The estimated EEMF at 800 r/min, compared with its theoretical value calculated from detected position, current, nominal inductance, and EMF constant according to (10), is shown in Fig. 8. From the figure, it is known that the observer is effective in estimating the EEMF and filtering the 12th harmonic component.

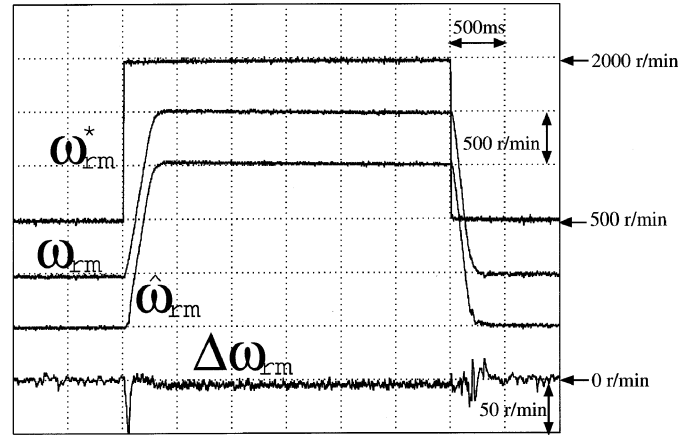


Fig. 10. Result of velocity control.

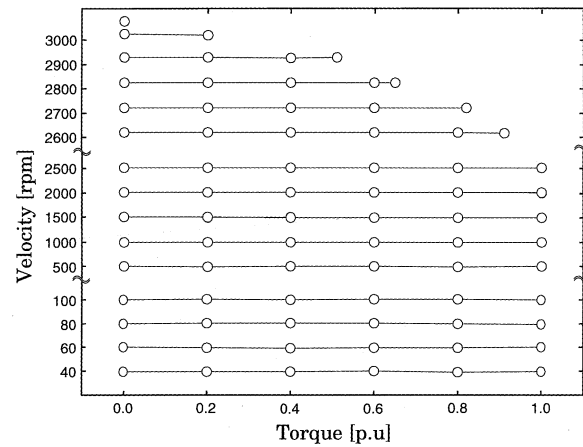


Fig. 11. Torque-velocity characteristics.

The estimated position $\hat{\theta}_{re}$ calculated from the phase of EEMF, compared with real position θ_{re} and position estimation error $\Delta\theta_{re} = \hat{\theta}_{re} - \theta_{re}$, is shown in Fig. 9. The maximum position estimation error is 1° . This may only lead to less than 1% of torque drop, which is a very good estimation.

The estimated velocity $\hat{\omega}_{rm}$ at mechanical angle, compared with velocity command ω_{rm}^* , detected velocity ω_{rm} and velocity estimation error $\Delta\omega_{rm} = \hat{\omega}_{rm} - \omega_{rm}$ at acceleration and deceleration between 500–2000 r/min without load, are shown in Fig. 10. From the figure, both the average velocity estimation error and control error are near zero, and at acceleration and deceleration, the velocity estimation error does not increase very much, which shows the effectiveness of the proposed pole assignment.

The velocity-torque characteristics are shown in Fig. 11. From the figure, the IPMSM can be controlled sensorlessly from 40 to 2500 r/min with 0%–100% load. It is also possible to control the motor sensorlessly up to 3050 r/min with field-weakening control. The maximum velocity control error is below 2% of the command velocity ω_{rm}^* .

VI. CONCLUSIONS

This paper proposed a new mathematical model for IPMSMs with the concept of EEMF defined. Based on the new model, a

disturbance observer proposed for SPMSMs was applied to an IPMSM for the position- and velocity-sensorless control. Because the proposed disturbance observer is based on a linear model for the IPMSM, its stability can be easily guaranteed and a robust control against velocity estimation error and higher order harmonic components can be realized by using linear control theories in the pole assignments. The proposed method was shown feasible by experiments.

As mentioned in Section II, the proposed new model is a general model for all the synchronous motors. Therefore, it makes a unified sensorless control for all the synchronous motors possible. Further research will be carried out on the possibility of SynRM's sensorless control using the proposed disturbance observer. In addition, attempts will also be made on standstill and low-speed drives of IPMSMs using the newly defined EEMF. The results will be reported later.

REFERENCES

- [1] A. Consoli, S. Musumeci, A. Raciti, and A. Testa, "Sensorless vector and speed control of brushless motor drives," *IEEE Trans. Ind. Electron.*, vol. 41, pp. 91–95, Feb. 1994.
- [2] C. French and P. Acarnley, "Control of permanent magnet motor drives using a new position estimation technique," *IEEE Trans. Ind. Applicat.*, vol. 32, pp. 1089–1097, Sept./Oct. 1996.
- [3] S. Ostlund and M. Brokemper, "Sensorless rotor-position detection from zero to rated speed for an integrated pm synchronous motor drive," *IEEE Trans. Ind. Applicat.*, vol. 32, pp. 1158–1165, Sept./Oct. 1996.
- [4] M. Tomita, T. Senjyu, S. Doki, and S. Okuma, "New sensorless controls for brushless dc motors using disturbance observers and adaptive velocity estimations," *IEEE Trans. Ind. Electron.*, vol. 45, pp. 274–282, Apr. 1998.
- [5] M. Schroedl, "Sensorless control of ac machines at low speed and standstill based on the "INFORM" method," in *Conf. Rec. 31th IEEE-IAS Annu. Meeting*, vol. 1, Oct. 1996, pp. 270–277.
- [6] T. Takeshita, M. Ichikawa, J. Lee, and N. Matsui, "Back emf estimation-based sensorless salient-pole brushless DC motor drives," *Trans. Inst. Elect. Eng. Jpn. D*, vol. 117, no. 1, pp. 98–104, Jan. 1997.
- [7] N. Kasa and H. Watanabe, "Position and speed sensorless control method for salient-pole brushless DC motor with estimated values correction," *Trans. Inst. Elect. Eng. Jpn. D*, vol. 117, no. 12, pp. 1488–1494, Dec. 1997.
- [8] H. Watanabe, T. Isii, and T. Fujii, "DC-brushless servo system without rotor position and speed sensor," in *Proc. IEEE IECON'87*, 1987, pp. 228–234.
- [9] M. J. Corley and R. D. Lorenz, "Rotor position and velocity estimation for a salient-pole permanent magnet synchronous machine at standstill and high speeds," *IEEE Trans. Ind. Applicat.*, vol. 34, pp. 784–789, July/Aug. 1998.
- [10] Z. Chen, M. Tomita, S. Doki, and S. Okuma, "The sensorless position estimation of salient-pole brushless dc motors and its stability," in *1998 Nat. Conv. Rec. IEEE-IAS*, vol. I, Aug. 1998, pp. 179–183.
- [11] G. Yang, R. Tomioka, M. Nakano, and T. Chin, "Position and speed sensorless control of brush-less dc motor based on an adaptive observer," *Trans. Inst. Elect. Eng. Jpn. D*, vol. 113, no. 5, pp. 579–586, May 1993.
- [12] Z. Chen, M. Tomita, S. Doki, and S. Okuma, "New adaptive sliding observers for position- and velocity-sensorless controls of brushless dc motors," *IEEE Trans. Ind. Electron.*, vol. 47, pp. 582–591, June 2000.



Zhiqian Chen (S'99–M'02) was born in Shanghai, China, in 1971. He received the B.E. degree in automatic control engineering from Southeast University, Nanjing, China, in 1994, and the M.E. and Ph.D. degrees in electrical engineering from Nagoya University, Nagoya, Japan in 1998 and 2001, respectively.

He is currently a Research Associate at Nagoya University. His research interest is sensorless control of synchronous motors.



Mutuwo Tomita (S'96–M'98) was born in Nagoya, Japan, in 1965. He received the B.E. degree from Mie University, Tsu, Japan, in 1988, and the M.E. and Ph.D. degrees from Nagoya University, Nagoya, Japan, in 1995 and 1998, respectively, all in electrical engineering.

He was an Electrical Engineering Teacher at Hamamatsu Jyohoku Technical Senior High School, Shizuoka, Japan, from 1988 to 1992, and at Inasa High School, Shizuoka, Japan, from 1992 to 1993. He is currently an Assistant Professor at Gifu

National College of Technology, Gifu, Japan. His research interest is brushless dc motors.



Shinji Doki (M'96) was born in Nagoya, Japan, in 1966. He received the B.E., M.E., and Ph.D. degrees in electronic-mechanical engineering from Nagoya University, Nagoya, Japan in 1990, 1992, and 1995, respectively.

He was an Assistant Professor at Nagoya University. Since June 2000, he has been an Associate Professor in the Department of Electrical Engineering, Mie University, Tsu, Japan. His research interests are power electronics and self-organized systems.

Dr. Doki received the IEEE IECON'92 Best Paper

Award.



Shigeru Okuma (M'82) was born in Gifu, Japan, in 1948. He received the B.E., M.E., and Ph.D. degrees in electrical engineering from Nagoya University, Nagoya, Japan, in 1970, 1972, and 1978, respectively. He also received the M.E. degree in systems engineering from Case Western Reserve University, Cleveland, OH, in 1974.

Since December 1990, he has been a Professor in the Department of Electrical Engineering, Nagoya University. His research interests are power electronics, robotics, and emergent soft computers.

Dr. Okuma received the IEEE IECON'92 Best Paper Award, as well as Paper Awards from the Japan Society for Precision Engineering and the Institute of Electrical Engineers of Japan.